Revista Mexicana de Física **40**, *No. 3 (1994) 447–458*

Three-dimensional gauging by electronic moiré contouring*

R. RODRÍGUEZ-VERA
Centro de Investigaciones en Optica, A.C.
Apartado postal 1–948, 37000 León, Guanajuato México

Recibido el 15 de diciembre de 1993; aceptado el 15 de febrero de 1994

ABSTRACT. Three-dimensional gauging involves the measurement and mapping of three-dimensional surfaces. Gauging accuracy depends on measurement accuracy in the images, image scale, and stereo-geometry. In industrial applications such as for quality control, multiple cameras are often needed to provide adequate stereoscopic coverage of the object. This paper reports an opto-electronic technique for obtain shape gauging from a diffuse object using just one camera. The surface to be measured is modulated by a linear fringe pattern that is projected using a conventional slide projector. In order to obtain a contour map of the surface, demodulation is carried out electronically producing a moiré pattern. Digital image processing by a computer, linked to the opto-electronic device is employed to determine the surface shape.

RESUMEN. La calibración tridimensional involucra la medida y mapeo de superficies tridimensionales. La exactitud de la calibración depende de la exactitud en las imágenes, de la escala y la estereogeometría. En aplicaciones industriales, tales como control de calidad, son frecuentemente necesarias varias cámaras para proporcionar un intervalo estereoscópico adecuado del objeto. Este artículo reporta una técnica optoelectrónica para obtener medición de forma de un objeto difuso, empleando sólo una cámara. La superficie a medir es modulada por un patrón de franjas lineal que son proyectadas usando un proyector de transparencias convencional. Con el fin de obtener un mapa de contornos de la superficie, la demodulación es llevada a cabo electrónicamente produciendo un patrón de moiré. Para determinar la forma de la superficie, se emplea procesamiento digital de imágenes mediante una computadora ligada al instrumento optoelectrónico.

PACS: 89.20.+a; 42.80.–f; 42.30.Va

1. INTRODUCTION

Gauging is an important process in manufacturing, and computer vision has already gained widespread applications for gauging in two dimensions. The ability of vision systems to perform 2-D measurement for process and quality control is one of the major impetuses for recent development of computer vision techniques [1]. The challenge in 3-D gauging is the development of hardware and software for automated operation to achieve the accuracy and speed that are usually needed in a manufacturing environment. Industrial measurement applications include many tasks that are time critical. While faster measurement techniques are always desirable, there are also certain levels of accuracy and repeatability that must be maintained.

*Part of this work was carried out at Loughborough University of Technology, England.

Three-dimensional gauging based on fringe projection has been known for a long time [2–8]. The most common methods involve projection of (a) optical interference fringes [2,3] or (b) a physical grating [4–8]. The former approach requires coherent light sources such as a laser to produce interference fringes obtained by the superposition of two plane wavefronts. The target surface is placed in the interference field in such way that the fringes are deformed accordcing to the shape of the surface. In the second approach (b), a grating is imaged on the surface target by using a conventional slide projector in white light illumination. The grating image is again deformed by the surface shape. A third method that uses coherent or incoherent illumination has been investigated by the author [9]. This approach is based on the Talbot effect, *i.e.*, the imaging of a periodic object without using an optical system (self-imaging). The Talbot image of a linear grating, in collimated illumination, is formed on the target that is spatially modulated by the shape of the surface. By imaging the deformed grating on a second grating placed on a plane displaced angularly with respect to the first, a contour map is created. The technique was used as a means to discriminate between hills and valleys of the object by using white light illumination [10]. This can be achieved by associating a different colour Talbot plane with a different plane of the target. One major disadvantage of this technique (as well as the interference fringe projection) is related to the object size to be tested. It must be at least the same size as the collimation optical system field.

In earlier work, moiré patterns had been formed by double exposure of the projected fringes onto photographic film [4]. The arrival of the low cost microcomputer, together with CCD-based opto-electronic system for fast detection of information, has left photographic techniques behind. Similar to the electronic speckle contouring (ESC) technique in electronic speckle pattern interferometry (ESPI) [11], fringe projection moiré can be used to obtain the topography of an object by "grid" contours [7,8], *i.e.*, a set of deformed lines superimposed on the surface target; and "depth" contours, a set of fringes whose depth is equidistant to a reference plane [4–6]. The first method requires direct processing of the deformed grating without using a second one. Projection moiré contouring where depth contours are obtained requires imaging of the deformed grating on a second reference grating.

Electronic moiré contouring (EMC) [12] is a technique based on the traditional projection moiré contouring technique, but with the variation that electronic demodulation is used to obtain the contour maps. This technique encodes the topographic information optically by projecting a linear grating on a surface target. The grating is deformed according to the target surface shape. Decodification is carried out by subtracting electronically the captured (by a CCD camera) encoded information between two different states of the target or with a reference grating, which can be generated by computer. The electronic apparatus, designed specially to work in a video ratio, is built up by A/D and D/A converters, a pass-band filter, an image subtractor, a rectifier, and a contrast stretcher. Putting all the parts together, a compact electronic system is constructed. The optical projection and capture systems and the electronic device plugged to a pc computer, conform the EMC setup. Experimental results indicate that the EMC technique may be extended as an industrial tool for quality control, or as feedback data in flexible manufacturing systems. In order to evaluate the EMC technique, fringe analysis was carried out by comparing fringe subtraction between reference and specimen gratings

using the electronic device and proprietary image processing equipment in a personal computer. A phase-stepping technique has been employed for data reduction, towards the full automation of the method.

2. THE EMC SYSTEM

Consider an target surface described by $z_1 = f_1(x, y)$ (Fig. 1). A linear grating whose rulings are perpendicular to the plane of the paper is projected on the surface. If the angle between the projection and viewing axes is β, the intensity distribution on the image plane is described by [4]

$$I_1(x, y, z) = A + B \cos \frac{2\pi}{p}[x \cos \beta - z_1 \sin \beta], \tag{1}$$

where A and B are constants and p is the grating period.

Consider a second target surface function $z_2 = f_2(x, y)$, which may represent a deviation from z_1 or the real target surface under test if z_1 is a flat, reference surface. Its intensity is

$$I_2(x, y, z) = A + B \cos \frac{2\pi}{p}[x \cos \beta - z_2 \sin \beta], \tag{2}$$

These intensity distributions, represented by voltage signals V_1 an V_2, are proportional to I_1 and I_2 respectively. The resulting processed video image is proportional to

$$\begin{aligned} V_1 - V_2 \propto |I_1 - I_2| &= B \cos \frac{2\pi}{p}[x \cos \beta - z_1 \sin \beta] - B \cos \frac{2\pi}{p}[x \cos \beta - z_2 \sin \beta] \\ &\cong K \sin \left[\frac{\pi}{p}(z_1 - Z_2) \sin \beta\right] \sin \frac{2\pi}{p}\left[x \cos \beta + \frac{(z_2 + z_1)}{2} \sin \beta\right], \end{aligned} \tag{3}$$

where K is a constant. Equation (3) represents the original projected fringe (except for a slight difference in phase) amplitude modulated by the factor

$$K \sin \left[\frac{\pi}{p}(z_1 - z_2) \sin \beta\right].$$

This modulation function corresponds to the moiré fringes and has a minimum wherever

$$\frac{\pi}{p}(z_2 - z_1) \sin \beta = n\pi,$$

where n is an integer, hence

$$\Delta z = (z_2 - z_1) = \frac{np}{\sin \beta}. \tag{4}$$

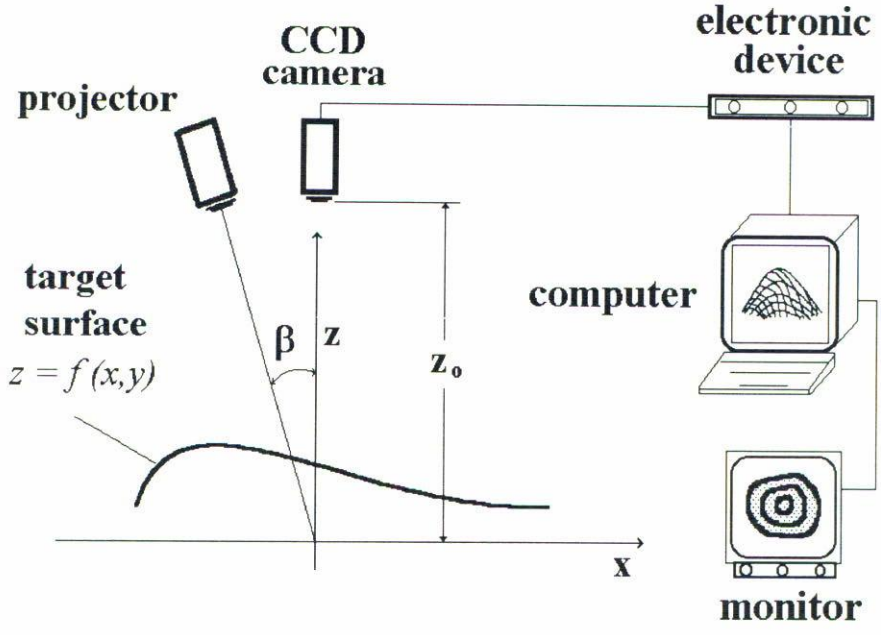

FIGURE 1. The EMC geometry.

The result is a moiré pattern representing a contour map of the surface $z_2 = f_2(x, y)$ with reference to the surface $z_1 = f_1(x, y)$, and with contour intervals given by Eq. (4). In the case where z_1 represents a flat surface the resultant moiré pattern will be a depth contour map of the surface z_2.

In order to use spherical illumination (which is used to practical condition for big object testing), it is necessary to make some corrections to Eq. (4). This was introduced by Gasvik and Fourney [13] and is given by

$$\Delta z = \frac{p_0}{\sin \beta_0} \left[\left(\sin \beta_0 + \frac{x}{z_2} \right)^2 + \cos^2 \beta_0 \right]^{1/2}, \tag{5}$$

where p_0 is the p value in the centre of the target surface which is the origin of the coordinate system, β_0 is the projection angle to the centre of the target and z_0 is the distance from the centre of the projection lens to the centre of the target. x is the distance along the target measured from the origin. It can be seen that for $x = 0$ or $z_0 \gg x$, Eq. (5) reduces to Eq. (4), in agreement with the given theory.

Figure 1 shows the experimental layout of the EMC system. A linear grating of period p is imaged obliquely at an angle β with respect to the viewing axis. A CCD camera images the target with the projected fringes; the result can be observed on a TV monitor connected to the electronic device output. This device is fed with a video signal from the TV camera which views the target surface and captures a first image of it. Subsequent images are subtracted from the first one at TV frame rate (30 Hz). The projector employed is a MP–1000 Newport Moiré Projector, which is mounted on a stage with a micrometer con-

FIGURE 2. Experimental results for absolute shape measuring: (a) contour map, (b) unwrapped phase map, and (c) wire-mesh isometric.

trolled transverse arrangement. The grating is fixed in the projector. The resultant image displayed on the monitor is an image of the target with moiré fringes superimposed upon it.

3. SOME APPLICATIONS

In the following sections, some applications of the EMC system will be described. These applications were simulated on real targets like plastic bottles, and thin plastic plates.

3.1. Example 1: Absolute shape measurement

For absolute shape measurement of a target, an image of a known, flat surface superimposed with projected fringes is captured in the electronic device. A 40 mm diameter spherical target is then replaced for the flat surface and its image is subtracted from that of the flat surface without altering the fringe projection layout. Fig. 2a is a photograph from the monitor of the contour map. In order to obtain the phase map and isometric plot from the contour map, the phase-stepping method is used [6]. Three contour patterns are captured: one at $-120°$, the second $0°$ and third shifted with respect to the last one by $+120°$. This is achieved by translating the projection system transversely with the micro-positioner. The translation is perpendicular to the projection axis, by $\frac{1}{3}(120°)$ of the grating pitch. Three intensity values I_1, I_2, and I_3 at each pixel location are used to compute the phase of the contour pattern from the relation [6]:

$$\phi = \arctan \frac{\sqrt{3}\,(I_3 - I_2)}{2I_1 - I_2 - I_3}. \tag{6}$$

Evaluating Eq. (6) at every pixel location transforms the three contour patterns into a modulo 2π (wrapped) phase distribution which is directly related to the shape of the surface. Fig. 2b and 2c show the phase map and isometric plot respectively.

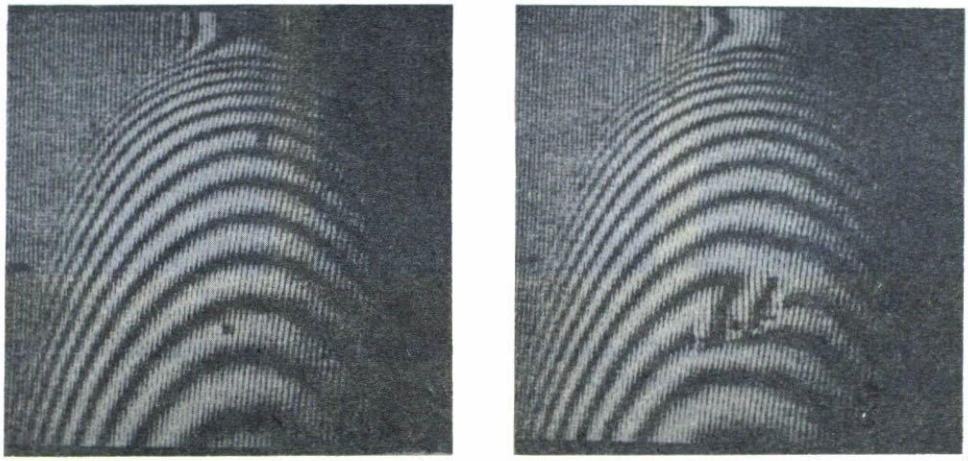

FIGURE 3. Defect detection for a quick inspection. Contour map obtained from a 2 litres plastic bottle: (a) without defect and (b) with defect.

3.2 Example 2: Surface inspection

Using the EMC system, surface defects can be detected and quantified. For quick inspection, a linear grating projected on a flat surface is stored. Replacement with the target under test and subsequent subtraction from the flat surface without altering the fringe projection layout, produces a contour map on the monitor. If a defect exists on the surface under test, the contour map will show it. Sudden changes on smooth contour fringes give an account of the defect. Figure 3 shows this situation for a 2 litre plastic bottle where the depth interval, Δz, was 3 mm. The physical difference that makes Figs. 3a and 3b different is a dent on the target surface. Obviously the surfaces under test may be continuous in order to detect the sudden changes on the fringe contours.

A quantitative analysis of defects may be achieved using the phase-stepping method. Following the same procedure as for shape measurements, a phase map and isometric plot are obtained and shown in Fig. 4. In this case the grating pitch on the target was 0.83 mm and $\beta = 32°$. The defect was identified as a 15×10 mm dent on the bottle surface with variable sinusoidal shape whose maximum depth was 2 mm.

In order to use the EMC method in on-line inspection, which may be useful to adapt in go/no-go controllers for industrial applications in quality control, other alternative surface inspection is described. This alternative makes possible qualitative comparisons between a "master" surface and a test specimen. A reference surface without defect and with superposed projected fringes is stored. The test surface is replaced at the same position without altering the projected fringe geometry. If this surface is free of defects, a dark field is to be seen on the monitor. If a defect exists or the surface is not identical to the reference one, the result is a moiré pattern showing this deviation. Figure 5 shows the

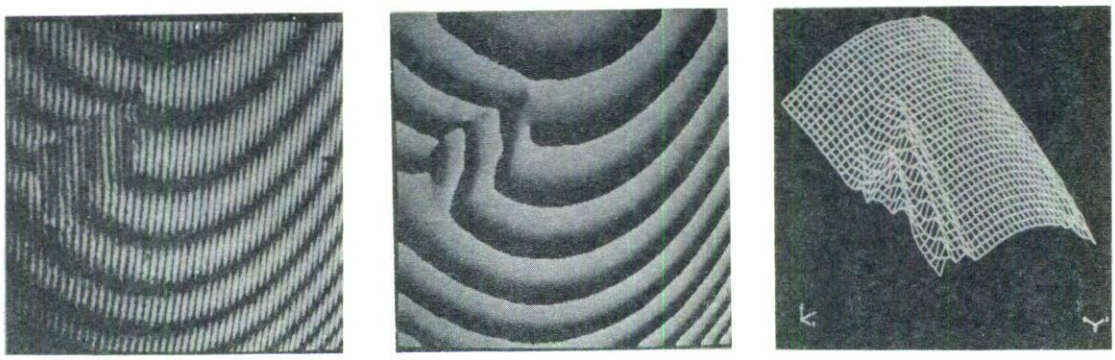

FIGURE 4. Quantitative results for defect measuring: (a) contour map, (b) unwrapped phase map, and (c) wire-mesh isometric.

FIGURE 5. Result obtained by comparing two bottles in the subtraction approach.

comparison between two plastic bottles with and without a defect. The result is clearly seen. The field around the defect is not dark because the reposition is not good enough. However, for a quick practical qualitative comparison, the result shown on the monitor screen is suitable.

It is necessary to mention that both of alternatives for surface inspection described above, are very useful in industrial environments. However, care will be necessary during the last alternative, since it is essential the repositioning of the test surface on the master one.

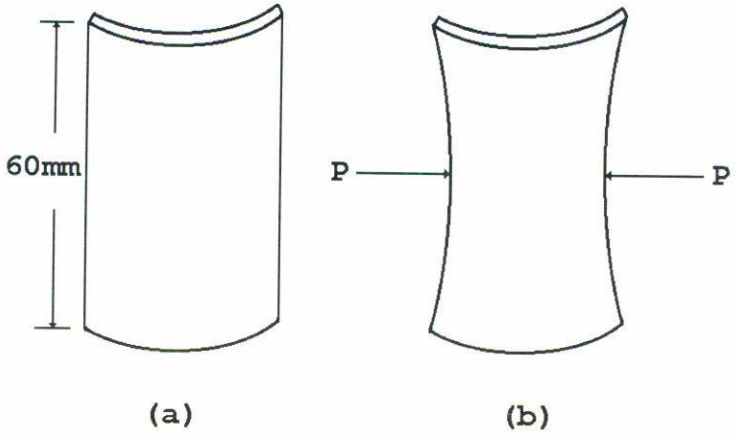

FIGURE 6. A thin plastic surface. (a) Initial cylindrical form, and (b) surface shape acquired by applying a load P.

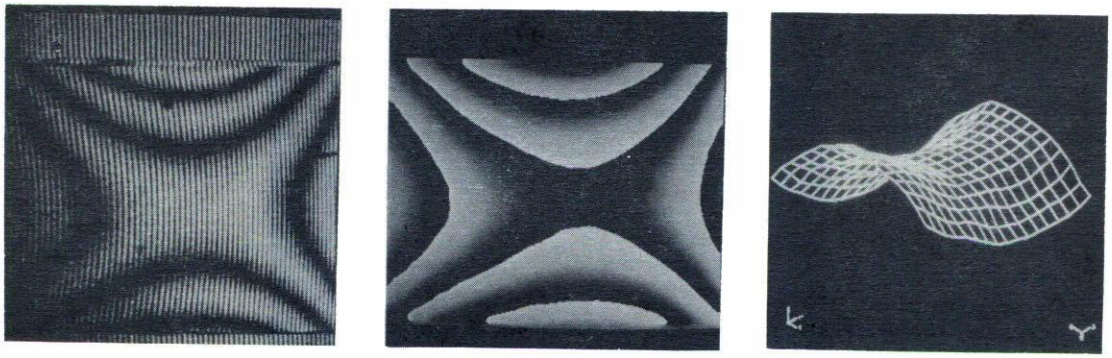

FIGURE 7. Final deformation result after the surface is loaded (a) contour map, (b) unwrapped phase map (c) final shape form.

3.3 Example 3: Deformation measurement

In order to demonstrate the possibility of extending the EMC technique to deformation measurement, a thin plastic cylindrical surface was tested. The dimensions of this cylinder are shown in Fig. 6a, where initially the surface is of 50 mm in radius and 60 mm in length. An image of this initial state of the shape with projected fringes on it is stored. A load P is applied to the middle part of the surface which produces a deformation depicted in Fig. 6b. Deformation contours appearing over the surface can be seen on the monitor. By using the usual phase-stepping procedure, the final acquired shape of the deformed target is obtained as seen in Fig. 7. In this case the contour interval is 2.5 mm which indicates that the larger deviation (centre of the target) from the original undeformed is 5 mm.

4. EVALUATION OF THE EMC TECHNIQUE

In order to obtain the required information, the depth of field of the viewing system in the EMC setup must be sufficient to cover the depth of the target surface. This is achieved by reducing the aperture of the viewing lens. However, the image of the grid contour is degraded by diffraction effects when the aperture is closed down. Also, the amount of light reaching the camera is less, then the signal to noise ratio is lower. The EMC technique was evaluated in terms of its visibility of the fringe contours. Image subtraction achieved by the electronic device of the EMC was compared with image subtraction carried out directly with a digital image processing card, the FG100 Image Pro sits on a pc buss. Also a comparison was made on the basis of the variation of the aperture of the vision system and the practical considerations of the television camera.

Figure 8 shows the intensity profile of a Ronchi grating projected on a flat surface. The images are captured for different aperture diameters (f–numbers) via the frame store (Fig. 8a) and without it, in direct form by the computer (Fig. 8b). The effect of the electronic device in EMC is noticed, in the truncation of the peaks in Fig. 8a. This is due to the electronic processing applied to the video signal. The electronic device is designed to work with high spatial frequency, it converts a variation of grating contrast to a variation in mean intensity improving the contrast in the output signal.

The band pass filter in the electronic device, is centered in 1.1 MHz and is used in order to minimize the random variations. This band pass filter helps to eliminate, in part, some of the carrier fringes. Also, included in the electronic device is the rectification and contrast stretching steps. In particular the rectification step produces a doubled carrier frequency. Grid contours obtained by projecting a grating on a flat and spherical target are shown in figs. 9a and 9b respectively. Depth contours in Fig. 9c correspond to a direct subtraction by the computer of the grid contours and 9d shows the depth contours obtained through the electronic device. Clearly is noticed in this last result how the electronic device nearly erases the doubled carrier frequency producing a better fringe contrast.

The adopted way of analyzing the contrast of an image is by measuring the standard deviation from its histogram. The standard deviation was measured for each contour map by varying the aperture size. A graphical comparison is shown in Fig. 10 for depth contours obtained through the frame store and directly by the computer. A higher contrast is found when electronic subtraction is performed compared to direct computer subtraction.

Solid state detector arrays, such as charged coupled devices (CCD's) cameras, are more frequent used for the image acquisition of fringe patterns. They consist of an accurate geometric screen containing light sensitive elements (pixels). The intensity incident on a pixel can be digitized and stored in discrete values in a computer memory. Normally intensity values are from 0 to 256. CCD's are chosen because the response at each pixel shows good linearity with the incident intensity.

Due to the finite number of intensity levels, a discrete sampling error may be made. Normally this discrete sampling error does not significantly influence the performance of the phase-stepping method. However, problems can arise when the contrast in the moiré fringe pattern is low. Then, with the electronic device, alleviate this situation in an inherent manner.

From Eq. (6) the phase $\phi(x, y)$ can be obtained. As a result of using the arctan function

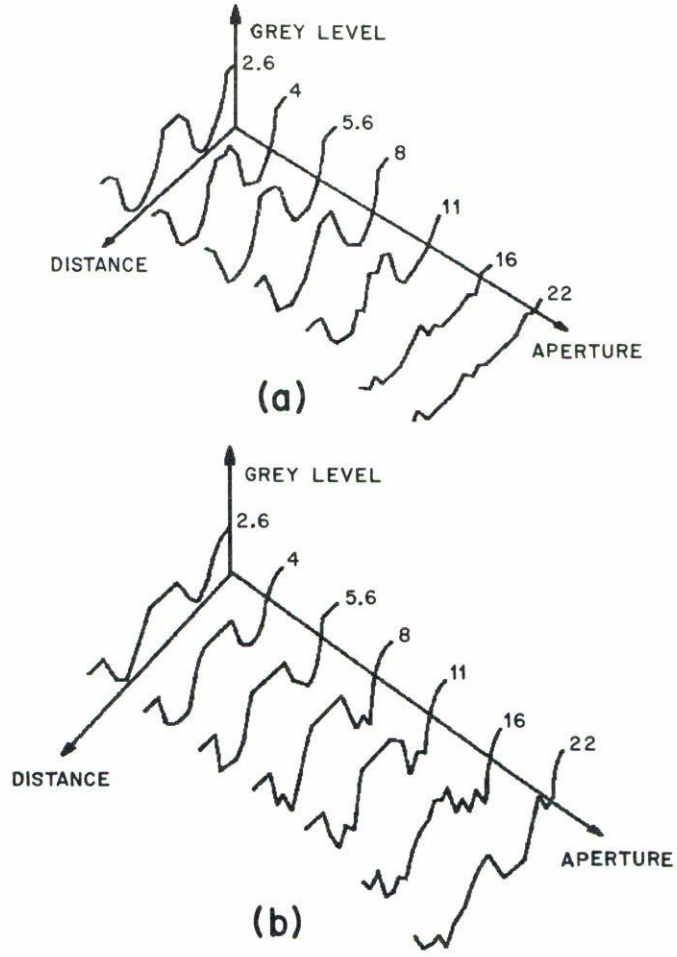

FIGURE 8. Image profile of a Ronchi grating projected on a flat surface. Captured images for different aperture sizes via: (a) direct and (b) electronic device.

the phase always lies between $-\pi$ and π. Since surfaces under consideration are supposed to be continuous, the continuous phase is obtained after compensating the phase jumps. To distinguish phase jumps from the object dependent phase difference in adjacent pixels theoretical more than two pixels per fringe must be acquired [14]. In the EMC case is applied this situation. The grid contours captured by the CCD must be separated at least two camera pixels, bearing in mind the camera lens resolution.

5. CONCLUSIONS

The potential of electronic moiré contouring linked to the phase-stepping method has been demonstrated experimentally. Absolute and comparative shape measurements have been carried out, in a simple and quick way to capture and retrieve information. Extension of EMC to surface deformation has shown that the technique can be used in a similar way to that of electronic speckle pattern interferometry (ESPI), with a reduced sensitivity. This

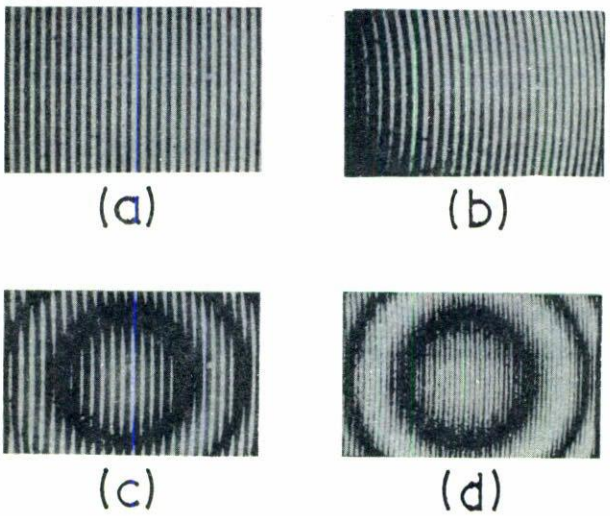

FIGURE 9. (a) and (b) grid contours generated by projecting a linear grating on a flat and spherical objects, respectively. Depth contours generated by subtracting the above grid contours via: (c) direct and (d) electronically.

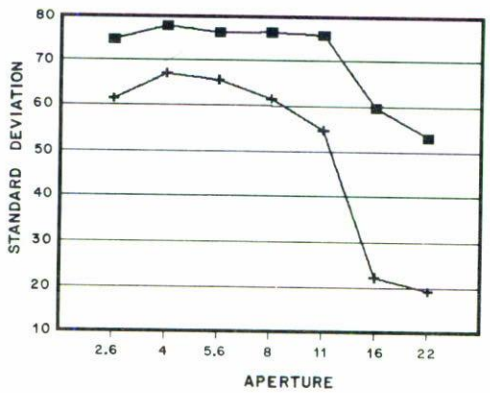

FIGURE 10. Contour contrast comparison produced (■) electronically and (+) using the computer.

is useful when measurement of large displacement or shape of big targets measurement is desired.

This method is very suitable for comparing the shape of different targets and therefore offers a powerful means for measuring the surface profile difference between a product specimen and a master target in real time. This is obtained by subsequent recording of the master and the product, resulting in a moiré pattern which maps the difference between the two targets due to, for example, manufacturing defects.

Finally it is necessary to mention that with conventional holographic or ESPI systems,

the contour interval obtained is of the order of λ, the wavelength of the light employed. Sometimes it is not necessary to use such a high sensitivity. For example, if big targets are tested, like car body panels, where defects of 1–5 mm on an area of 1 square meter or more exist, the EMC technique is far better for carrying out such testing.

ACKNOWLEDGEMENTS

I would like to thank Dr. D. Kerr for his useful comments and suggestions, Mr. K. Topley for producing the photographic material, and Mrs. J. Redman for the line drawings, all of them from Loughborough University of Technology, Department of Mechanical Engineering, England. The financial support provided by CONACyT is gratefully acknowledged.

REFERENCES

1. A. Novini, *Proc. SPIE* **1526** (1991) 2.
2. P.O. Varman, *Opt. and Lasers in Eng.* **5** (1984) 41.
3. M.R. Morshedizadeh and C.M. Wykes, *J. Phys. E: Sci. Instrum.* **22** (1989) 88.
4. J.D. Hovanesian and Y.Y. Hung, *Appl. Opt.* **10** (1971) 2734.
5. K.J. Gasvik, *Appl. Opt.* **22** (1983) 3543.
6. G.T. Reid, R.C. Rixon, and H.I. Messer, *Opt. and Laser Technol.* **16** (1984) 315.
7. M. Halioua and H.C. Liu, *Opt. and Lasers in Eng.* **11** (1989) 185.
8. M. Takeda and K. Mutoh, *Appl. Opt.* **22** (1983) 3977.
9. R. Rodriguez-Vera, D. Kerr, and F. Mendoza-Santoyo, *J. Mod. Opt.* **38** (1991) 1935.
10. R. Rodriguez-Vera, D. Kerr, and F. Mendoza-Santoyo, *Proc. SPIE* **1553** (1991) 55.
11. R. Rodriguez-Vera, D. Kerr, and F. Mendoza-Santoyo, *J. Opt. Soc. Am.* **9A** (1992) 2000.
12. R. Rodriguez-Vera and D. Kerr, in *Proc. of Int. Conference Fringe Analysis'92*, Leeds University, England (16-17 Sept., 1992) p. 31.
13. K.J. Gasvik and M.E. Fourney, *J. Appl. Mech.* **53** (1986) 652.
14. J.E. Greivenkamp and J.H. Bruning, in *Optical Shop Testing*, D. Malacara, Ed. Wiley Series in Pure and Applied Optics, John Wiley and Sons, New York (1992) chapter 14.